Title:
Modeling of microstructure in the HAZ for microalloyed steel S700 MC

Sub title:
Modeling of grain growth in HAZ

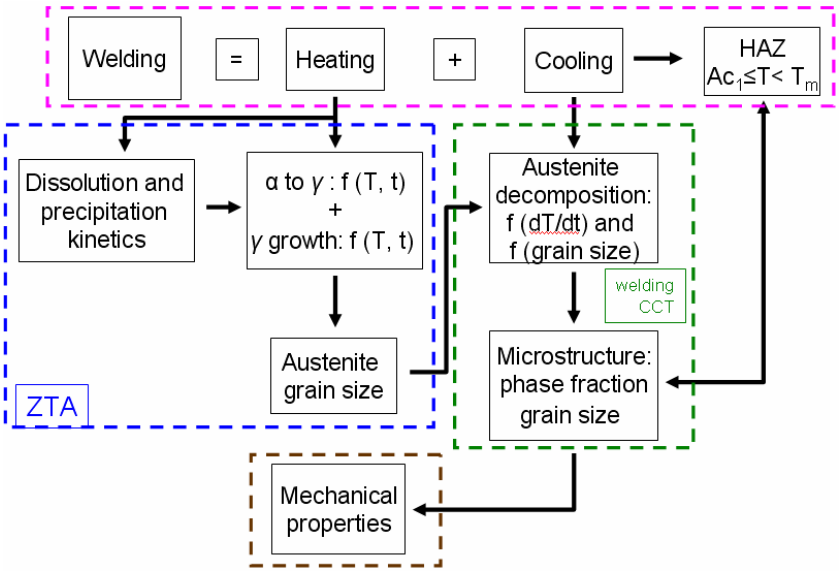

Autor: Mizanur Rahman	Projekt: Join4+, 1.1	Datum: 10.01.2011

Dokumentnummer: HJB_GG_20101221_M. Rahman_Version_01

1. Introduction

The heat affected zone (HAZ) of modern TM steels can soften in the presence of weld thermal cycle, even at the relatively low heat input during MAG welding. The HAZ is one of the most common regions of weld failure due to the stress concentration and the reduction of strength. Since the softening mechanism in HAZ can vary from steel to steel because of their chemical compositions and production process, the newly developed TM steel, S700 MC should be carefully investigated in order to achieve adequate strength in the weld HAZ. It is very important to know the degree and extension to which this softening takes place, given the nature of the base metal and the welding conditions.

Some TMCP steels such as X70 and X80, HAZ softening is often the results of high heat input welding procedure because of slow heat dissipation in the HAZ [1]. For higher grade TM steel, HAZ softening can happen even under moderate heat input because of the base metal's ultra fine grain size and its bainite and martensite dominated microstructure [2].

The objective of this Dissertation work is to develop a numerical model for the prediction of HAZ softening in HS microalloyed steel S700 MC. The HAZ can be defined as the temperature between Ac_1 and the melting temperature. In some steels, the softening can also happen at the region below Ac_1 temperature, which is called annealing softening.

During heating in the welding process, the α-*γ* transformation takes place above Ac_1 temperature and the transformation completes, when the temperature reaches Ac_3. In general the austenite grains start growing above Ac_3 temperature and the growth rate can be controlled as a function of peak temperature in HAZ.

During cooling the grain growth still continues till the temperature reaches approximately Ac_3 and the *γ*- α transformation takes place afterwards. A new microstructure evolves as a result of welding thermal cycles. The mechanical properties can then be characterized based on new grain sizes and phase fractions in the HAZ.

An approach for the modeling of HAZ / soft zone is described in the Figure 1. The whole model can be subdivided into four groups; a) calculating of welding thermal cycle, b) modeling of austenite grain size and c) austenite decomposition and d) mechanical properties calculation based on microstructure evolved in HAZ. In this work, both modeling groups a) and b) are discussed.

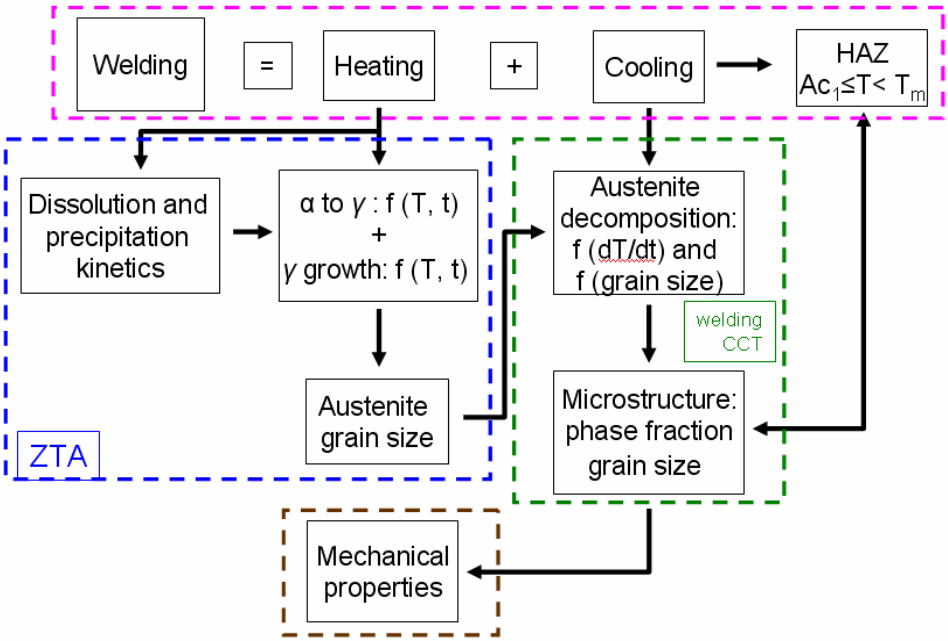

Figure 1: An approach for microstructure modeling in HAZ

1.1 Austenite grain growth and literature study

Weld strength is a dominating factor in assessing the overall performance of the HS microalloyed steels, which, to a large degree, is controlled by the austenite grain size in the heat affected zone (HAZ) [3]. Large austenite grains near the fusion line may promote the formation of martensitic or bainitic transformation products with adverse effects on weld properties, e.g., fracture toughness [4-5]. Austenite grain growth in the weld HAZ is therefore, an important factor to determine the microstructure and mechanical properties of the weld. Austenite grain size also influences the kinetics of phase transformation during the cooling cycle [6].

1.1.1 Modeling of isothermal grain growth

In 1948, Beck [7] first introduced a general form of an empirical model for isothermal grain growth in pure metals and solid-solution alloys.

$$D^{1/n} - D_0^{1/n} = K_1 t \qquad \textbf{Equ. 1}$$

where, D - average grain size, D_0 - initial grain size, n - time exponent for growth and K_1 - growth constant. Both n and K_1 are functions of temperature. If $D_0 << D$, D_0 can be neglected. The equ. [1] then can be expressed as follows and n and K can be experimentally evaluated

$$D = Kt^n \qquad \textbf{Equ. 2}$$

The rate of grain growth can be obtained by differentiating of equ. [2] and eliminating t. According to equ. [3], it is shown that the grain growth is dependent on instantaneous grain size [8].

$$\frac{dD}{dt} = nK^{\frac{1}{n}}\left(\frac{1}{D}\right)^{\frac{1}{n}-1} \qquad \textbf{Equ. 3}$$

In 1953 C.S. Smith [9] established a reciprocal relationship between average grain size, *D* and grain boundary surface area. For isothermal growth of random grains, the equ. [3] may be rewritten as

$$\frac{dD}{dt} = K'\left(\frac{\gamma}{D}\right)^{\frac{1}{n}-1} \qquad \textbf{Equ. 4}$$

where, *K'* is a new temperature dependent parameter and *γ* is surface grain boundary energy (J/m^2). The expression is thus consistent with the concept that the driving force for grain growth is the boundary surface free energy per unit volume. In 1969 H. Hu and B. B Rath [10] again established a grain growth relation with driving force

$$\frac{dD}{dt} = M\left(\Delta F\right)^m \qquad \textbf{Equ. 5}$$

where, *M* (m^4/J.sec) is the mobility of grain growth, *ΔF* is driving pressure (N/m^2) and *m* is driving pressure exponent. The mobility, *M* can be expressed as an Arrhenius type equation.

$$M = M_0 \exp\left(-Q/RT\right) \qquad \textbf{Equ. 6}$$

where, M_0 is mobility constant, *Q*-activation energy, *R*-gas constant and *T* is temperature. As equ. [4] and [5] are dimensionally consistent and of the same form [10], they are empirically valid. By comparing equ. [4] and [6], the following relations can be made. The grain growth equation can now be expressed as in equ. [9].

$$m = \frac{1}{n} - 1 \qquad \textbf{Equ. 7}$$

$$\Delta F = \frac{\gamma}{D} \qquad \textbf{Equ. 8}$$

$$\frac{dD}{dt} = M_0 \exp\left(-Q/RT\right)\left(\frac{\gamma}{D}\right)^m \qquad \textbf{Equ. 9}$$

1.1.1.1 Effect of second phase particles

C. Smith [11] outlined the fundamental principles of interpretation of microstructures in terms of the equilibrium between phases and grain interfaces. Grain boundary motion can be inhibited by the presence of insoluble, incoherent second phase spherical particles. The surface area of grain boundary deceases, when a boundary intersects a particle. Zener proposed that a pinning (drag) pressure exerted by the particles on the boundary would encounter the driving pressure for grain growth due to the curvature of the grain boundary. The Zener drag, P_z is determined from the equ. [10].

$$P_z = \frac{3\gamma}{2} \cdot \frac{f}{r} \qquad \textbf{Equ. 10}$$

where, f is the volume fraction of particles and r is particle radius. The resulting driving force, ΔF_R for grain growth in the presence of particles can be derived by subtracting P_z from ΔF in the equ. [8].

$$\Delta F_R = \Delta F - P_z \qquad \textbf{Equ. 11}$$

The grain growth equation can now be established with considering second phase particles and written as

$$\frac{dD}{dt} = M_0 \exp\left(-Q/RT\right)\left(\frac{\gamma}{D} - \frac{3\gamma}{2}\frac{f}{r}\right)^m \qquad \textbf{Equ. 12}$$

In 1998 P.A. Manohar [12] studied published literatures comprehensively and properly investigated some unclear parameter definitions, which were found the previous grain growth models. He established then two other possible relationships among driving force, grain boundary energy and grain size.

$$\Delta F = \frac{2\gamma}{D} \text{ or } \Delta F = \frac{4\gamma}{D} \qquad \textbf{Equ. 13}$$

Therefore, the equ. [12] can be expressed in a general form for isothermal grain growth by including two arbitrary constants; a and b, where a = 1 to 4 and b = 3/2 in this case.

$$\frac{dD}{dt} = M_0 \exp\left(-Q/RT\right)\gamma^m\left(\frac{a}{D} - b\sum\frac{f}{r}\right)^m \qquad \textbf{Equ. 14}$$

1.1.2 FE model for isothermal and non-isothermal grain growth

A model for non-isothermal grain growth can be developed on the basis of an isothermal grain growth model using additivity rule [13]. S. Denis [14] developed a model for the analysis of the transformation kinetics during continuous heating or cooling based on an isothermal model and on the rule of additivity. The thermal cycles were subdivided into small successive isothermal time steps.

S. Jiao et al [13] approximated the experimental reheating curves by a series of isothermal steps in which every steps had the same duration Δt. The grain size d_{i+1} was calculated during the time interval Δt by means of equ. [15], where no pinning effects were considered.

$$d_{i+1} = \left[d_0^n + K_1\left(t_{i+1}^* + \Delta t\right)\exp\left(K_2 / T_{i+1}\right)\right]^{1/n} \qquad \textbf{Equ. 15}$$

where $t_{i+1}^* = \dfrac{d_i^n - d_0^n}{K_1 \exp\left(K_2 / T_{i+1}\right)}$, K_1 and K_2 are material constants

In the present work, a FE model has been developed on the basis of continuous differential equation for isothermal grain growth as described in equ. [14]. The growth rate, *dD/dt* can be approximated using an explicit. The discretized growth rate is given in equ. [16] and the equ. [14] can now be expressed as in the equ. [17].

$$\frac{dD}{dt} = \frac{D^{k+1} - D^k}{\Delta t}, \text{ where } \Delta t = t^{k+1} - t^k \qquad \textbf{Equ. 16}$$

$$D^{k+1} = D^k + \Delta t\left[M_0 \exp\left(-Q / RT^k\right)\gamma^m\left(\frac{a}{D^k} - b\sum\frac{f}{r}\right)\right]^m \qquad \textbf{Equ. 17}$$

The grain size, D^{k+1} is calculated numerically during each time step Δt from equ. [17]. At the beginning, when Δt=0, the grain size D^k is assumed as the initial grain size, D_0 and $D^{k+1} = D^k = D_0$. The temperature, T^k is taken as initial temperature, T_0.

A new temperature, T^k is calculated in each time step iteratively, which is then employed in the grain growth model to calculate new grain size. The final grain size, D^{k+1} can be obtained with the accumulation of grain sizes calculated in each time step.

$$D^{k+1} = D^k + \Delta t\left[M_0 \exp\left(-Q / RT^k\right)\gamma^m\left(\frac{a}{D^k} - b\sum\frac{f}{r}\right)\right]^m \qquad \textbf{Equ. 18}$$

2. Austenite grain growth simulation

The calculation of austenite grain growth in the case of isothermal or non-isothermal heat treatment for steel is not new. Since many decades, researchers have worked on this field with a great interest. All steels do not behave in the same manner even they are treated with the same thermal cycles. The grain growth kinetics is therefore, different from each other. P. A. Manohar et al [15] described an empirical model and predicted isothermal grain growth for C-Mn, C-Mn-V, C-Mn-Ti and C-Mn-Nb steels and found good correlation between experimental and calculated results. M. Shome et al [16] and O. M. Akselsen et al [17] proposed analytical approaches for grain growth in HAZ. Many others like J. Moon [6] incorporated the effect of Zener pinning in the model and predicted the austenite grain size in HAZ for Ti-microalloyed steel. Very recently K. Banerjee et al [3] studied non-isothermal austenite grain growth kinetics for X80 linepipe steel under the influence of several combinations of microalloying elements; Nb, Ti and Mo. In both works of J. Moon and K. Banerjee, non-isothermal austenite formation and austenite grain growth have been investigated at high heating rates to various austenitization temperatures. In addition to microstructural characterization by conventional metallographic techniques, the evolution of the particle size distribution has been investigated by transmission electron microscopy. Based on the experimental data, a phenomenological model for non-isothermal austenite grain growth kinetics is proposed taking into account the dissolution kinetics of precipitates. The dissolution model is coupled to the grain growth model via a Zener-type pinning force that depends on particle radius and volume fraction which is already derived in equ. [14].

2.1 Implementation of grain growth model in Sysweld software

In this study, a 2D FE-model was conducted in Sysweld and the phenomenological model for austenite grain growth established in equ. [17] was implemented. The objective of this simulation is to verify the functionality of the implemented model. A condition has been applied in the model in terms of the value of resulting driving pressure. The grain growth can be completely inhibited, when the resulting driving pressure became zero or negative. Unless and otherwise, the grain growth ia allowed.

2.1.1 Grain growth simulation

A welding thermal cycles have been simulated using Goldak [18] double ellipsoid volumetric heat source. The Goldak parameters are listed in Table 1.

Table 1: Goldak parameters for simulation of thermal cycles in HAZ

Front intensity q_f	Rare intensity q_r	a_f (mm)	a_r (mm)	b (mm)	c (mm)	v (mm/sec)	kJ/cm
1.5	1.0	8.0	12.0	4.0	5.5	5.0	6.0

The precipitation kinetics data, mainly the volume fraction and particles coarsening behavior required for grain growth simulation were taken form J. Moon [6]. The volume fraction was calculated using Thermo-calc. As shown in Figure 2 (left), the particle volume fraction decreases with increasing temperature because the stability of the particle decreases at high temperature, which leads to particle dissolution. The LSW (Lifshitz, Slyovoz and Wagner) equation was used [19] to predict the particle size evolution. Figure 2 (right) shows the coarsening behavior of TiN particle predicted by J. Moon. TiN particles are stable till very high temperature. All other parameters used for grain growth simulation are listed in Table 2.

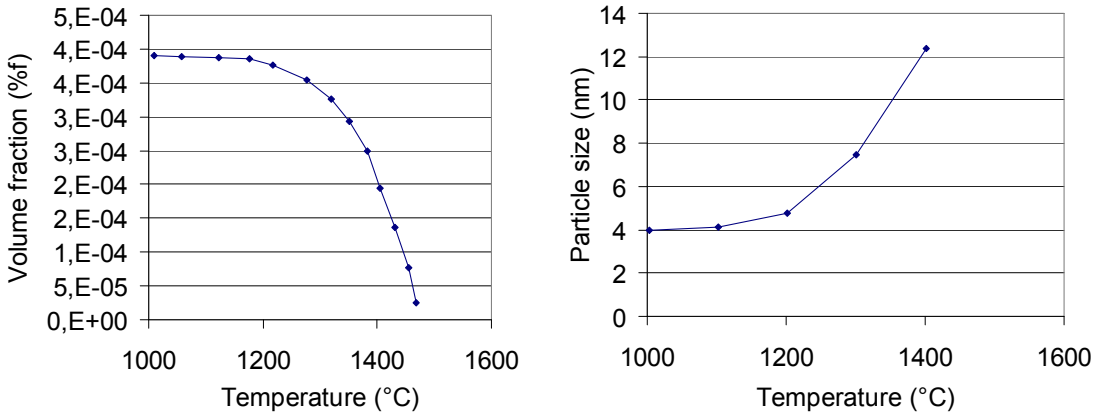

Figure 2: Calculated volume fraction of TiN (left) and particle coarsening behavior (right) during continuous heating and cooling [6]

Table 2: Parameters for grain growth simulation

D_0 (µm)	n	Q (J/mol)	R (J/mol.K)	M_0 (µm^4/J.sec)	γ (J/µm^2)	a	b
10	0.5	312000	8.3	8.5e+24	0.86e-12	2	1.5

2.1.2 Simulation results

Contour plots for the simulated temperature field and grain size distribution were presented in Figure 3. The simulated results showed that the grain growth could take place at the temperature above approximately 950 °C. Although the initial grain size was assumed 10µm, the calculated minimum grain size was 3.3µm as shown in the contour plot. This reduction of grain size occurred only in the boundary elements, which is still a mistake present in the implementation of the FE-model for austenite grain growth. The wrong statement in the programming for conversion of calculated grain size from the integration points to the element nodes may be the reason of this failure.

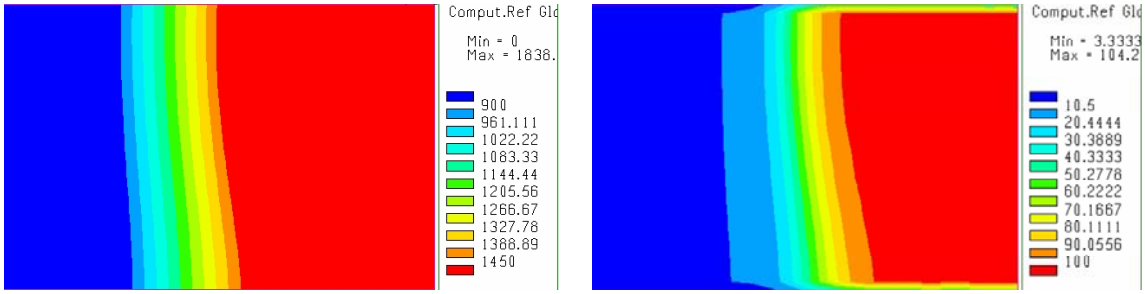

Figure 3: Contour plot for temperature field (left) and grain size distribution (right)

Figure 4 represented the grain size distribution in HAZ as a function of thermal cycles. It could be reported that the austenite grain growth would mainly continue during heating in the welding process. Both the driving pressure for grain boundary, ΔF and the ratio f/r so called Zener drag, P_z were reduced, but ΔF still became higher than P_z.

An assumption was made in the simulation that the particle volume fraction and particle radius could go back to 0their original conditions during cooling. As a result, P_z would get higher during cooling, but ΔF remained same as the end of heating cycle. Therefore, the tendency of the resulting driving pressure would go negative, which could stop the grain growth during cooling although the temperature was higher than the grain growth starting temperature, 950 °C. The simulated results are compared with the experimental results from J. Moon [6] and shown in Figure 5.

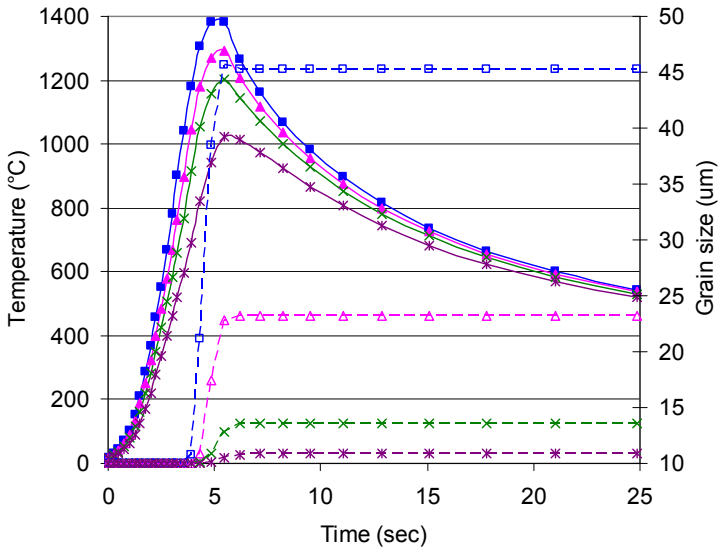

Figure 4: Simulated grain growth in HAZ as a function of thermal cycle; temperature in solid line and grain size in broken line

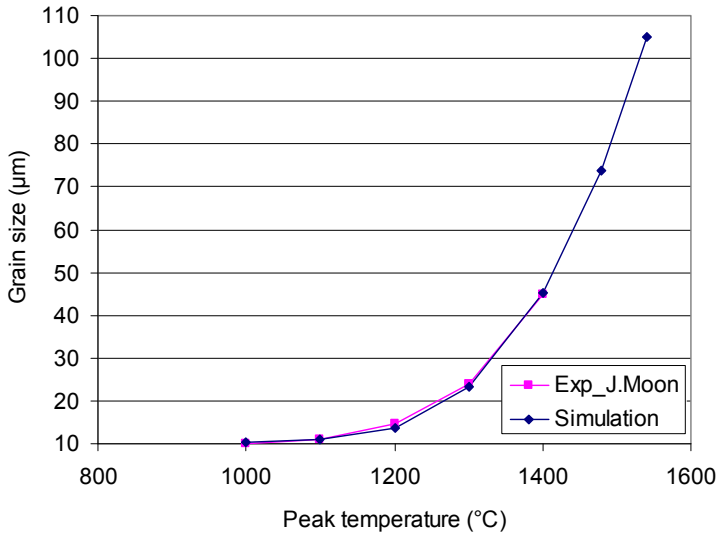

Figure 5: Comparison between experimental and simulated grain size distribution in HAZ

3. The determination of prior austenite grain size

To measure the austenite grain size metallographically, it is essential to reveal the austenite microstructure in the as-quenched samples. The experiments were performed using Dilatometer DL805. The samples were heated up to 1100°C and isothermally socked for 10sec and quenched using Helium gas. The quenched samples were ground and polished using conventional metallographic techniques. Both standard Nital 3% and Oberhoffer Etchants were used to reveal the austenite grain boundaries. Polished and etched samples were then photographed using an optical microscope. The results are shown in Figure 6. Satisfactory results were not achieved. The prior-austenite grains are not clearly visible. The experimental investigation is still running to improve the results.

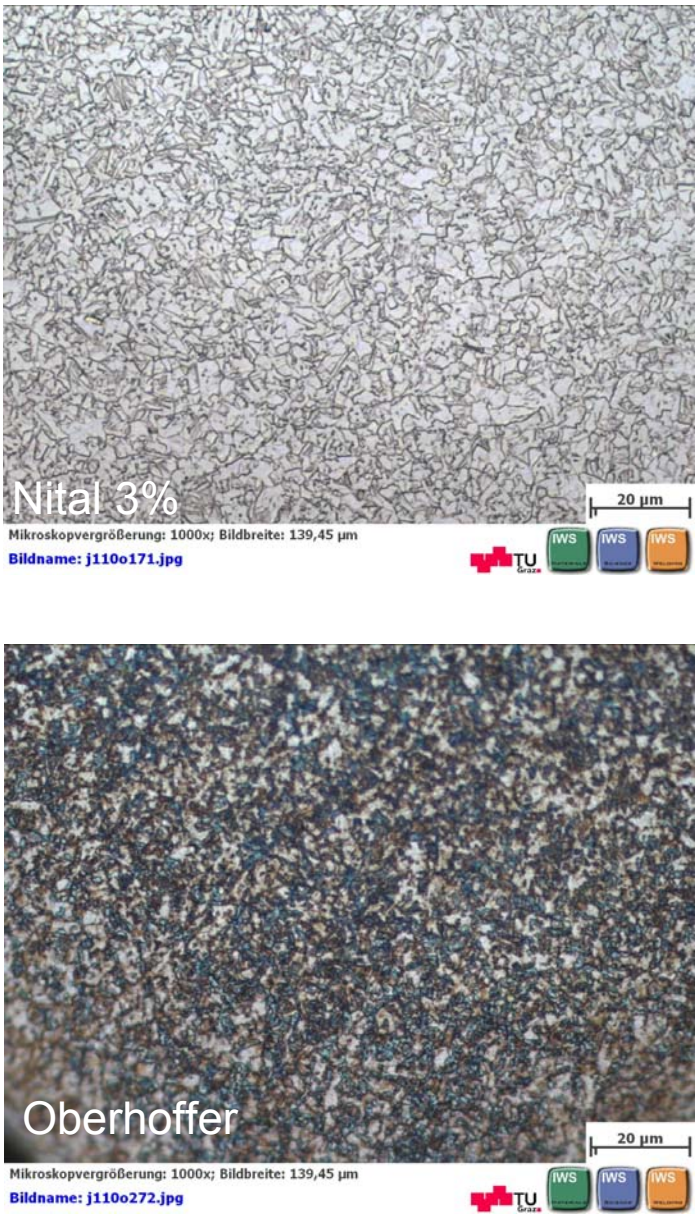

Figure 6: Metallography for the measurement of austenite grain size

4. Conclusion

- An overall modeling concept has been described for the microstructure evolution in the HAZ
- A literature study on grain growth models has been performed
- The isothermal grain growth model has been approximated and a FE- explicit model for non-isothermal grain growth has been developed
- The grain growth model has been successfully implemented in Sysweld software, which can predict both isothermal and non-isothermal austenite grain growth with or without considering the effects of Zener pinning
- The simulated grain size distribution in the HAZ show good agreement with the experimental results published in J. Moon [6]
- The Dilatometry has been performed to measure the prior austenite grain size using different etching methods, but clear results are not found. The further improvement is currently going on

5. Outlook

- The conversion of calculated results from the integration points to boundary nodes are necessary to be improved
- Proper Etchants and metallographic techniques will be applied for experimental measurement of prior-austenite grain size
- The precipitation kinetics will be studied and a Matcalc simulation will be performed to calculate the evolution of particle volume fraction and radius for steels S700 MC
- The grain growth simulation will be performed using the implemented grain growth model for steels S700 MC

6. Reference

1 N. Yurioka, TMCP Steels and their welding, *Welding in the World*, Vol. 35, No. 6, pp. 375-390, 1995

2 Y. Chen et al, Microstructure modeling of HAZ softening in microalloyed high strength linepipe steels, *ISOPE*, pp. 3001-3006, 2007

3 K. Banerjee, et al, Non-isothermal Austenite Grain Growth Kinetics in a Microalloyed X80 Linepipe Steel, *Metallurgical and Materials Transactions A* , DOI: 10.1007/s11661-010-0376-2, 2010

4 N.J. Grant, *J. Met*. Vol. 35, pp. 20–27, 1983

5 L.P. Zhang, et al, *Metallurgical and Materials Transactions A* , Vol. 30A, pp. 2089–2096, 1999

6 J. Moon et al, Prediction for the austenite grain size in the presence of growing particles in the weld HAZ of Ti-microalloyed steel, *Materials Science and Engineering A*, Vol. 459, pp. 40–46, 2007

7 P.A Beck et al, AIME Trans, Vol. 175, pp. 372-394, 1948

8 P.A Beck et al, Effect of recrystallized grain size on grain growth, *Phy. Rev*, Vol. 75, pp. 526-527, 1948

9 C.S Smith at el, *AIME Trans.*, Vol. 197, pp. 81-87, 1953

10 H. Hu and B.B. Rath, On the time exponent in isothermal grain growth, *Metal. Trans*. Vol. 1, pp. 3181-3184, 1969

11 C.S. Smith, Trans. AIME, Vol. 175, pp. 15, 1948

12 P. A. Manohar et al, Five Decades of the Zener Equation, *ISIJ International*, Vol. 38. No. 9, pp. 913-924, 1998

13 S. Jiao et al, The modelling of the grain growth in the continuous reheating process of a low carbon Si-Mn Bearing TRIP steel, ISIJ International, Vol. 40, No. 10, pp. 1035-1040, 2000

14 S. Denis, Mathematical model coupling phase transformations and temperature evolutions in steel, ISIJ Int., Vol. 32, pp. 316, 1992

15 P A Manohar, Grain growth predictions in microalloyed steels, *ISIJ International*. Vol. 36, No. 2, pp. 194-200, 1996

16 M. Shome, A modified analytical approach for modelling grain growth in the coarse grain HAZ of HSLA steels, *Scripta Materialia,* Vol, 50, pp. 1007–1010, 2004

17 O. M. Akselsen et al, HAZ grain growth mechanisms in welding of low carbon microalloyed steels, *Acta metal*. Vol. 34, No. 9, pp. 1807-1815, 1986

18 J. Goldak et al, A new finite element model for welding heat sources, *Metallurgical Transactions B*, Vol. 15B, pp. 299-305, 1984

19 J. Moon et al, Acta Metall., Vol. 54, pp. 1053-1061, 2006